

Two Distinct Conformers of the Cyclic Heptapeptide Phakellistatin 2 Isolated from the Fijian Marine Sponge *Stylotella aurantium*

Jioji N. Tabudravu,[†] Marcel Jaspars,^{*,†} Linda A. Morris,[†]
J. Jantina Kettenes-van den Bosch,[‡] and Nigel Smith[§]

Marine Natural Products Laboratory, Department of Chemistry, University of Aberdeen,
Old Aberdeen, Scotland, UK, Department of Biomolecular Mass Spectrometry,
Utrecht Institute for Pharmaceutical Sciences, Utrecht University, Utrecht, The Netherlands, and
Paterson Institute for Cancer Research, Christie Hospital NHS Trust, Manchester, UK

m.jaspars@abdn.ac.uk

Received July 18, 2002

The isolation, structure determination, and solution conformation of two conformers of the cyclic heptapeptide phakellistatin 2 (*cyclo*-[Phe¹-*cis*-Pro²-Ile³-Ile⁴-*cis*-Pro⁵-Tyr⁶-*cis*-Pro⁷]) isolated from the Fijian marine sponge *Stylotella aurantium* are reported. The conformers can be isolated separately by HPLC and are stable in methanol solution over a period of weeks as determined by NMR. Their NMR spectra and mass spectral fragmentation patterns differ significantly. Their solution conformations were determined by NOE-restrained molecular dynamics calculations and indicated that the two conformers had different folds, hydrogen bonding patterns, and solvent accessible surfaces. These factors may contribute to the independent stability of the two conformers, and may explain the variable biological activity previously reported for phakellistatin 2.

Introduction

Many biologically active proline-rich cyclic peptides have been isolated from marine sponges, for example, the hymenamides,^{1–4} stylopeptide,⁵ the axinellins,^{6,7} the axinastatins,^{8–10} and the phakellistatins.^{11–17} Cyclic pep-

tides are favored by Nature as they are less prone to enzymatic degradation and have a higher bioavailability and a greatly reduced conformational flexibility.¹⁸ This reduced conformational flexibility is the result of the restricted angle ϕ of proline residues. Proline-rich cyclic peptides often have a well-defined conformation in solution, which may be the reason behind the observed bioactivity.^{19,20}

We have previously reported the isolation and structure determination of two new proline-rich cyclic peptides,^{21,22} as well as two known ones^{7,11} from the Fijian marine sponge *Stylotella aurantium* (Order Halichondrida; Family Halichondriidae). In this paper we describe the isolation of two distinct conformers of the known proline-rich cyclic heptapeptide phakellistatin 2 (*cyclo*-[Phe¹-*cis*-Pro²-Ile³-Ile⁴-*cis*-Pro⁵-Tyr⁶-*cis*-Pro⁷], **1**). The initial isolation of this compound was performed by Pettit and co-workers from the Indian Ocean marine sponge *Phakellia carteri*, and the compound was found to have

* To whom correspondence should be addressed. Phone: +44 1224 272895. Fax: +44 1224 272921.

[†] University of Aberdeen.

[‡] Utrecht University.

[§] Christie Hospital NHS Trust.

(1) Kobayashi, J.; Tsuda, M.; Nakamura, T.; Mikami, Y.; Shigemori, H. *Tetrahedron* **1993**, *49*, 2391–2402.

(2) Tsuda, M.; Shigemori, H.; Mikami, Y.; Kobayashi, J. *Tetrahedron* **1993**, *49*, 6785–6786.

(3) Tsuda, M.; Sasaki, T.; Kobayashi, J. *Tetrahedron* **1994**, *50*, 4667–4680.

(4) Kobayashi, J.; Nakamura, T.; Tsuda, M. *Tetrahedron* **1996**, *52*, 6355–6360.

(5) Pettit, G. R.; Srirangam, J. K.; Herald, D. L.; Xu, J.; Boyd, M. R.; Cichacz, Z.; Kamano, Y.; Schmidt, J. M.; Erickson, K. L. *J. Org. Chem.* **1995**, *60*, 8257–8261.

(6) Randazzo, A.; Piazz, F. D.; Orru, S.; Debitus, C.; Roussakis, C.; Pucci, P.; Paloma, L. G. *Eur. J. Org. Chem.* **1998**, 2659–2665.

(7) Kong, F.; Burgoyne, D. L.; Andersen, R. J. *Tetrahedron Lett.* **1992**, *33*, 3269–3272.

(8) Pettit, G. R.; Herald, C. L.; Boyd, M. R.; Leet, J. E.; Dufresne, C.; Doubek, D. L.; Schmidt, J. M.; Cerny, R. L.; Hooper, J. N.; Rutzler, K. C. *J. Med. Chem.* **1991**, *34*, 3339–3340.

(9) Pettit, G. R.; Gao, F.; Cerny, R. *Heterocycles* **1993**, *35*, 711–717.

(10) Pettit, G. R.; Gao, F.; Schmidt, B.; Chapuis, J.; Cerny, R. L. *Biorg. Med. Chem. Lett.* **1994**, *4*, 2935–2940.

(11) Pettit, G. R.; Tan, R.; Williams, M. D.; Tackett, L.; Schmidt, J. M.; Cerny, R. L.; Hooper, J. N. A. *Biorg. Med. Chem. Lett.* **1993**, *3*, 2869–2874.

(12) Pettit, G. R.; Xu, J.; Cichacz, Z. A.; Williams, M. D.; Chapuis, J. C. *Biorg. Med. Chem. Lett.* **1994**, *4*, 2677–2682.

(13) Pettit, G. R.; Xu, J.; Cichacz, Z.; Schmidt, J. M.; Dorsaz, A. C. *Heterocycles* **1995**, *40*, 501–506.

(14) Pettit, G. R.; Xu, J.; Cichacz, Z.; Williams, M. D.; Dorsaz, A. C.; Brune, D. C. *Biorg. Med. Chem. Lett.* **1994**, *4*, 2091–2096.

(15) Pettit, G. R.; Cichacz, Z.; Barkoczy, J.; Dorsaz, A. C.; Herald, D. L.; Williams, M. D.; Doubek, D. L.; Schmidt, J. M.; Tackett, L. P.; Brune, D. C. *J. Nat. Prod.* **1993**, *56*, 260–267.

(16) Pettit, G. R.; Tan, R.; Herald, D. L.; Cerny, R. L.; Williams, M. D. *J. Org. Chem.* **1994**, *59*, 1593–1595.

(17) Pettit, G. R.; Cichacz, Z.; Barkoczy, J.; Dorman, A. C.; Herald, D. L.; Doubek, D. L.; Schmidt, J. M.; Tackett, L. P.; Brune, D. C.; Cerny, R. L.; Hooper, J. N.; Bakus, G. J. *J. Nat. Prod.* **1993**, *56*, 260–267.

(18) Wipf, P. *Chem. Rev.* **1995**, *95*, 2115–2134.

(19) Kessler, H.; Bats, J. W.; Lautz, J.; Muller, A. *Liebigs Ann. Chem.* **1989**, 913–928.

(20) Mechnich, O.; Hessler, G.; Kessler, H. *Helv. Chim. Acta* **1997**, *80*, 1338–1353.

(21) Tabudravu, J. N.; Morris, L. A.; Kettenes van den Bosch, J. J.; Jaspars, M. *Tetrahedron Lett.* **2001**, *42*, 9273–9276.

(22) Tabudravu, J. N.; Morris, L. A.; Kettenes van den Bosch, J. J.; Jaspars, M. *Tetrahedron* **2002**, *58*, 7863–7868.

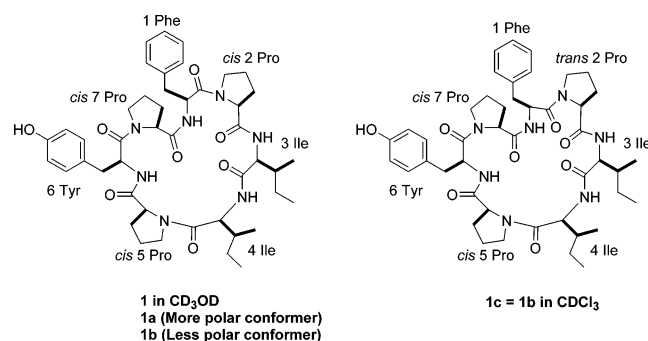
a submicromolar ED_{50} against P388 cells. However, this activity could not be reproduced upon reisolation of the compound.¹¹ A synthesis of **1** seemed to indicate that the original structure might have been miss-assigned.²³ A later re-synthesis of the compound by Pettit et al. indicated that the structure originally proposed was in fact correct, but that the original bioactivity could not be attributed to it.²⁴

Isolation

The CH_2Cl_2 partition fraction of our Fijian collection of *Stylotella aurantium* showed IC_{50} values of 0.47 and 0.45 $\mu g/mL$ for A2780 ovarian tumor and K562 leukaemia cancer cells, respectively. Size exclusion chromatography of this fraction, followed by reversed-phase HPLC yielded the new compounds wainunamide²¹ and axinellin C,²² as well as the known compounds pseudoaxinellin⁷ and phakellistatin 2 (**1**).¹¹ In addition, a seemingly new compound was also isolated. Its HPLC retention time indicated that it was slightly less polar than phakellistatin 2.

Structure Determination

The more polar compound (**1a**), as inferred from its retention time on reversed-phase HPLC, was found to be phakellistatin 2 (**1**), with an accurate mass measurement of m/z 850.4421 ($[M + Na]^+ \Delta 0.0$ mmu from that calculated for $C_{45}H_{62}N_7O_8$). The ^{13}C and DEPT-135 spectrum of phakellistatin 2 exhibited seven amide carbonyls and seven α -methine carbons characteristic of a heptapeptide. The amino acid composition of phakellistatin 2 was established after detailed analysis of 1H , ^{13}C , COSY, HSQC, HMBC, and HSQC-TOCSY data obtained in CD_3OD . It showed the presence of one phenylalanine, three prolines, one tyrosine, and two isoleucine residues (Table S1). The NMR data are identical with those reported for the initial isolation¹¹ and the later re-synthesis²⁴ of phakellistatin 2. The amino acid composition was confirmed by HPLC analysis of the acid hydrolysate.



The amino acid sequence was confirmed by combination of both ROESY and ESI- MS^n data. The ROESY spectrum cross-peaks $Phe^1-H\alpha/Pro^2-H\alpha$, $Ile^4-H\alpha/Pro^5-H\alpha$, and $Tyr^6-H\alpha/Pro^7-H\alpha$ provided evidence of these connectivities and indicated that all three proline amide bonds adopted the cis geometry. This geometry was further

supported by the difference in ^{13}C NMR chemical shifts of $Pro^2\Delta\delta_{C\beta-C\gamma} = 8.8$ ppm, $Pro^5\Delta\delta_{C\beta-C\gamma} = 9.7$ ppm, and $Pro^7\Delta\delta_{C\beta-C\gamma} = 9.1$ ppm, which is indicative of the presence of cis peptidic bonds.^{25,26}

The MS spectrum of phakellistatin 2 contained the signals at m/z 828 $[M + H]^+$ and m/z 850 $[M + Na]^+$. The ESI- MS^n spectra of the $[M + H]^+$ and $[M + Na]^+$ of **1a** indicated the preferential ring opening at the Phe^1-Pro^2 peptide bond (Figure 1a,b) or the Tyr^6-Pro^7 peptide bond (Figure 1c). The $[M + Na]^+$ initially showed a loss of the Phe^1 CO, followed by loss of a Pro^2 and then successive losses of Ile^3 and Ile^4 (Figure 1a), which confirmed the NMR-based proposal that the two Ile residues were adjacent in the sequence. The remaining fragment m/z 499 can be attributed to $[Pro^5-Tyr^6-Pro^7-Phe^1 - CO]$. Additional fragmentation of the $[M + H]^+$ (Figure 1b,c) indicated the full sequence to be *cyclo*($Phe^1-cis-Pro^2-Ile^3-Ile^4-cis-Pro^5-Tyr^6-cis-Pro^7$). Chiral TLC of the acid hydrolysate revealed all the amino acid residues to be L.

The structure determination of the less polar compound (**1b**), as judged by its greater retention time on reversed-phase HPLC compared to phakellistatin 2, began with its accurate mass measurement of 828.4594 ($[M + H]^+ \Delta 0.7$ mmu from that calculated for $C_{45}H_{62}N_7O_8$). Analysis of $^1H-^1H$ COSY, HSQC, HMBC, and HSQC-TOCSY experiments obtained in CD_3OD revealed spin systems corresponding to one phenylalanine, three prolines, one tyrosine, and two isoleucine residues (Table 1), as in phakellistatin 2. The amino acid composition was confirmed by HPLC analyses of the acid hydrolysate. Since only 18 degrees of unsaturation could be accounted for by the functionality present in the seven individual amino acids, it was apparent that this compound was also a cyclic peptide.

The amino acid sequence was established by combination of T-ROESY and ESI- MS^n fragmentation data. The T-ROESY spectrum cross-peaks $Phe^1-H\alpha/Pro^2-H\alpha$, $Ile^4-H\alpha/Pro^5-H\alpha$, and $Tyr^6-H\alpha/Pro^7-H\alpha$ provided evidence of these connectivities as well as indicating that the Pro^2 , Pro^5 , and Pro^7 amide bonds adopted the cis geometry. This was supported further by the difference of ^{13}C NMR chemical shifts of $Pro^2\Delta\delta_{C\beta-C\gamma} = 9.4$ ppm, $Pro^5\Delta\delta_{C\beta-C\gamma} = 9.2$ ppm, and $Pro^7\Delta\delta_{C\beta-C\gamma} = 9.2$ ppm, indicative of the presence of a cis peptidic linkage. At this stage there was evidence for fragments Phe^1-Pro^2 , Ile^4-Pro^5 , and Tyr^6-Pro^7 . An HMBC correlation $Pro^7-CO/Phe^1-H\beta_{AB}$ combined two of these fragments to give $Tyr^6-Pro^7-Phe^1-Pro^2$, but additional sequence information needed to be derived from the mass spectral fragmentation patterns.

The mass spectrum of this compound contained m/z 828 $[M + H]^+$ and m/z 850 $[M + Na]^+$. The ESI- MS^n of these ions showed different fragmentation patterns from the more polar compound (Figure 2). In two cases the ring opening occurred at a proline peptide bond, Tyr^6-Pro^7 (Figure 2b) and Pro^2-Ile^3 (Figure 2c). In the other case the ring opening occurred at Pro^7-Phe^1 (Figure 2a). The ring opening was not found to occur at Phe^1-Pro^2 , the favored ring opening position for **1a**. One of the pathways for **1b** (Figure 2b) started with the loss of 260 corresponding to the loss of Pro^5-Tyr^6 followed by the loss of 113 (Ile^4) followed by 210 (Leu^3-Pro^2) and leaving an

(23) Mechnich, O.; Kessler, H. *Lett. Pept. Sci.* **1997**, 4, 21–28.

(24) Pettit, G. R.; Rhodes, M. R.; Tan, R. *J. Nat. Prod.* **1999**, 62, 409–414.

(25) Dorman, D. E.; Borvey, F. A. *J. Org. Chem.* **1973**, 38, 1719.

(26) Dorman, D. E.; Borvey, F. A. *J. Org. Chem.* **1973**, 38, 2379.

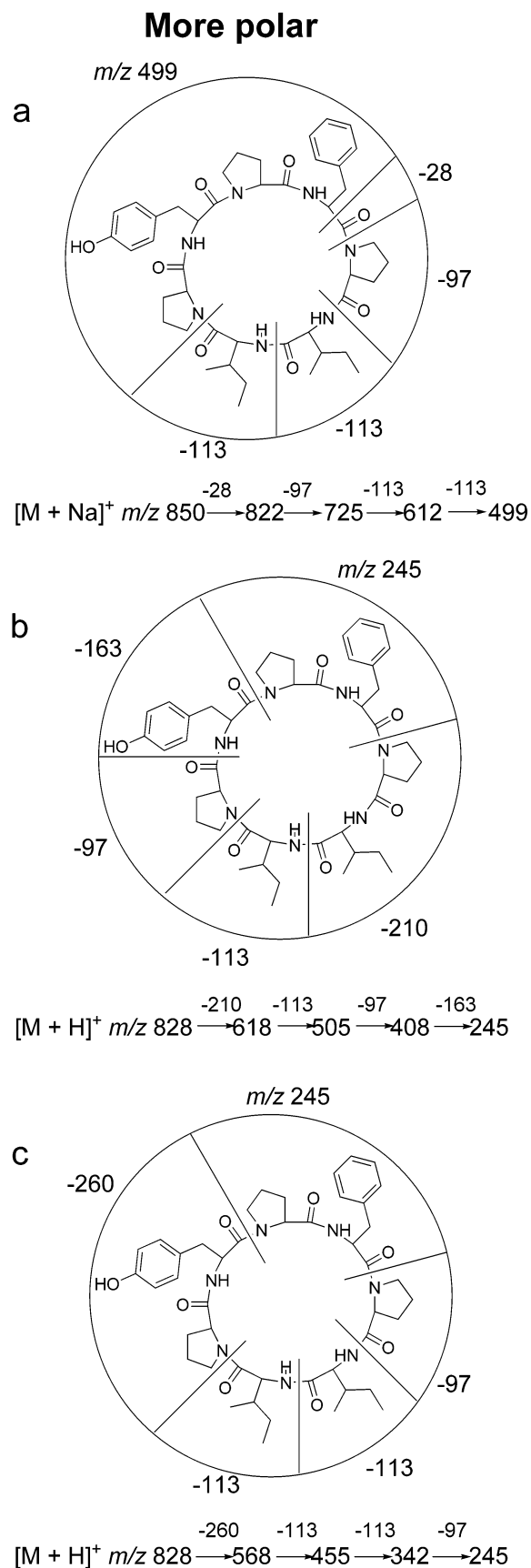


FIGURE 1. Major fragmentation pathways of **1a** (more polar conformer) in ESI-MSⁿ. In part a, m/z 499 is $[M + Na]^+$; in parts b and c, m/z 245 is $[M + H]^+$.

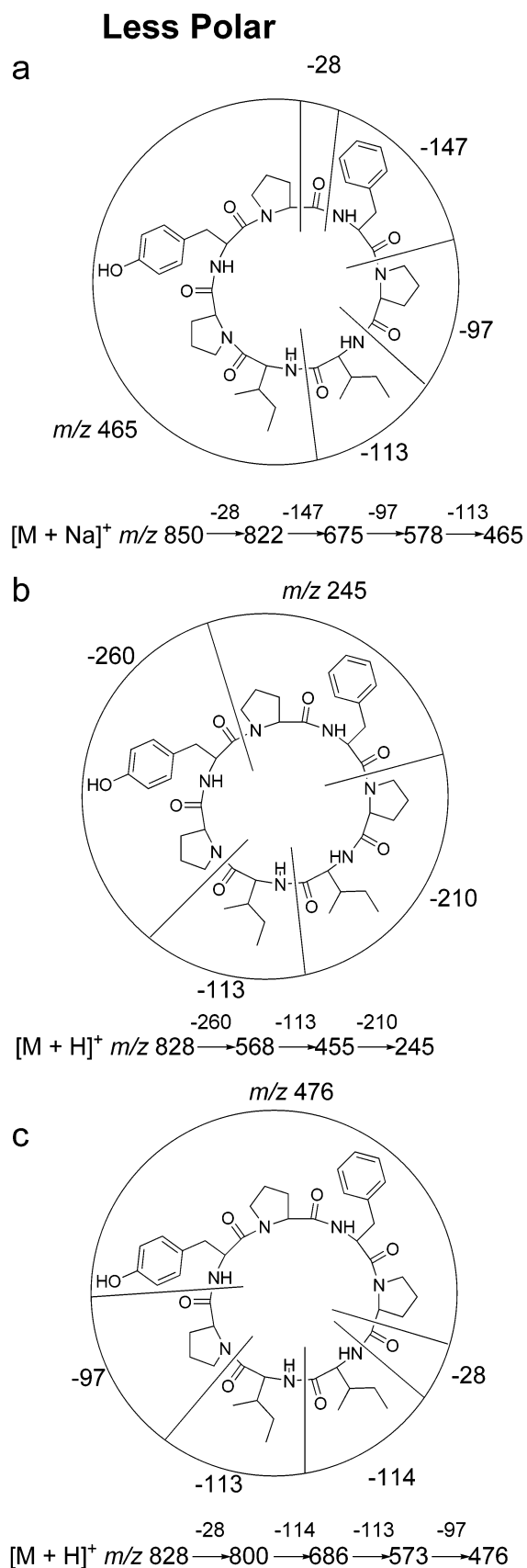


FIGURE 2. Major fragmentation pathways of **1b** (less polar conformer) in ESI-MSⁿ. In part 2a, m/z 465 is $[M + Na]^+$; in part b, m/z is $[M + H]^+$; in part c, Ile³ fragments incorporating an extra proton.

TABLE 1. ^1H (δ /ppm, Proton Count, Multiplicity, J (Hz)), 400 MHz, ^{13}C (δ /ppm, Multiplicity), 100 MHz, and 2D NMR Data in CD_3OD for the Phakellistatin 2 Less Polar Conformer (**1b**)

no.	residue	atom	^{13}C	^1H	COSY $^1\text{H}-^1\text{H}$	HMBC C \rightarrow H
1	Phe	α	52.9 (d)	4.58 (1H, m)	H1 β_{B} , NH1	
		β	39.2 (t)	A. 2.98 (1H, m) B. 2.90 (1H, m)	H1 α	H1 α , H1(2/6), H1 β_{A} , H1 β_{B}
		1	137.2 (s)			H1 β_{A} , H1 β_{B} , H1(2/6)
		2/6	129.5 (d)	7.27 (1H, d, 8.0)	H1(3/5), H1(4)	H1(2/6), H1(3/5)
		3/5	128.0 (d)	7.16 (2H, d, 8.4)	H1(2/6), H1(4)	H1(4)
		4	130.0 (d)	7.22 (1H, d, 9.6)	H1(2/6), H1(3/5)	
		CO	172.4 (s)			H1 α , H2 α , H2 β_{B}
		NH		6.71 (1H, d, 8.3)	H1 α	
2	Pro	α	62.1 (d)	3.49 (1H, m)	H2 β_{B}	H2 γ_{A}
		β	31.6 (t)	A. 1.69 (1H, m) B. 1.28 (1H, m)	H2 α	
		γ	22.2 (t)	A. 1.55 (1H, m) B. 1.38 (1H, m)	H2 δ_{B}	H2 α
		δ	47.0 (t)	A. 3.39 (1H, m) B. 3.13 (1H, m)	H2 δ_{B} H2 γ_{A} , H2 δ_{A}	H2 β_{A}
		CO	172.6 (s)			
		α	59.6 (d)	3.89 (1H, d, 10.4)	H3 β , NH3	3 γCH_3
		β	35.4 (d)	1.89 (1H, m)	H3 α , 3 γCH_3	H3 α , 3 γCH_3 , 3 δCH_3
		γ	26.6 (t)	A. 1.41 (1H, m) B. 1.12 (1H, m)	H3 γ_{B} , 3 γCH_3 H3 γ_{A} , 3 γCH_3	H3 α , 3 γCH_3 , 3 δCH_3
3	Ile	γCH_3	15.9 (q)	0.76 (3H, d, 6.8)	H3 β , H3 γ_{B}	
		δCH_3	10.5 (q)	0.81 (3H, d, 7.2)	3 γCH_3	
		CO	172.6 (s)			H3 α
		NH		9.31 (1H, d, 7.4)	H3 α	
		α	58.3 (d)	3.98 (1H, d, 7.6)	H4 β , NH4	H4 β , 4 γCH_3
		β	37.2 (d)	1.74 (1H, m)	H4 α , 4 γCH_3 , 4 δCH_3	H4 α , 4 δCH_3 , H4 γ
		γ	26.2 (t)	A. 1.70 (1H, m) B. 1.31 (1H, m)	4 δCH_3 , 4 γCH_3	H4 α
		γCH_3	15.1 (q)	0.96 (3H, d, 6.8)	H4 β	H4 γ_{A} , H4 γ_{B}
4	Ile	δCH_3	10.8 (q)	0.92 (3H, d, 6.8)	H4 β , H4 γ_{A}	
		CO	174.1 (s)			H4 α
		NH		8.42 (1H, d, 9.7)	H4 α	
		α	62.5 (d)	4.41 (1H, m)	H5 β_{B}	H5 β_{B}
		β	31.8 (t)	A. 2.43 (1H, m) B. 2.02 (1H, m)	H5 α , H4 β_{B} , H4 γ_{B} H5 β_{A}	H5 α , H5 δ_{A}
		γ	22.6 (t)	A. 1.91 (1H, m) B. 1.64 (1H, m)	H5 γ_{B} H5 β_{A} , H4 γ_{A}	H5 α , H5 β_{A} , H5 β_{B}
		δ	47.6 (t)	A. 3.52 (1H, m) B. 3.42 (1H, m)	H5 δ_{B} H5 δ_{A}	H5 α , H5 β_{A} , H5 β_{B}
		CO	172.8 (s)			H5 α , H5 β_{A} , H5 β_{B}
5	Pro	α	62.5 (d)	4.41 (1H, m)	H5 β_{B}	H5 β_{B}
		β	31.8 (t)	A. 2.43 (1H, m) B. 2.02 (1H, m)	H5 α , H4 β_{B} , H4 γ_{B} H5 β_{A}	H5 α , H5 δ_{A}
		γ	22.6 (t)	A. 1.91 (1H, m) B. 1.64 (1H, m)	H5 γ_{B} H5 β_{A} , H4 γ_{A}	H5 α , H5 β_{A} , H5 β_{B}
		δ	47.6 (t)	A. 3.52 (1H, m) B. 3.42 (1H, m)	H5 δ_{B} H5 δ_{A}	H5 α , H5 β_{A} , H5 β_{B}
		CO	172.8 (s)			H5 α , H5 β_{A} , H5 β_{B}
		a	54.0 (d)	4.53 (1H, m)	H6 β , NH6	H6(2/6), H6 β
		b	37.0 (t)	2.97 (1H, m)	H6 α	H6(3/5)
		1	127.1 (s)			H6(2/6)
6	Tyr	2/6	131.5 (d)	6.76 (2H, d, 8.4)	H6(2/6)	H6(2/6)
		3/5	115.7 (d)	6.59 (2H, d, 8.8)	H6(3/5)	H6(2/6), H6(3/5)
		4	157.3 (s)			H6(2/6), H6(3/5)
		CO	170.1 (s)			H6 α , H6 β
		NH		6.89 (1H, obs)	H6 α	
		α	59.2 (d)	4.45 (1H, m)	H7 β_{A}	H7 γ_{B}
		β	31.4 (t)	A. 2.04 (1H, m) B. 1.88 (1H, s)	H7 α	H7 δ_{A}
		γ	22.2 (t)	A. 2.05 (1H, m) B. 1.78 (1H, m)		H7 α
7	Pro	δ	47.8 (t)	A. 3.52 (1H, m) B. 3.32 (1H, m)	H7 δ_{B} H7 δ_{A}	H7 α
		CO	172.4 (s)			H1 β_{A} , H1 β_{B}

m/z of 245 corresponding to $\text{Pro}^7\text{-Phe}^1$. Complementary to this are the fragmentation pathways indicated in parts a and c of Figure 2 with m/z 465 ($\text{Ile}^4\text{-Pro}^5\text{-Tyr}^6\text{-Pro}^7$) and m/z 476 ($\text{Tyr}^6\text{-Pro}^7\text{-Phe}^1\text{-Pro}^2 - \text{CO}$). The proposed sequence of **1b** from 2D NMR data and ESI-MSⁿ was therefore established as *cyclo*($\text{Phe}^1\text{-cis-Pro}^2\text{-Ile}^3\text{-Ile}^4\text{-cis-Pro}^5\text{-Tyr}^6\text{-cis-Pro}^7$), identical to **1a**. Chiral TLC of the acid hydrolysate revealed all the amino acid residues to be L. Therefore, this less polar compound, **1b**, has the same sequence and absolute stereochemistry as **1a**.

This less polar variant of phakellistatin 2 was also examined in CDCl_3 (**1c**, Table 2) and it was found that

the NMR data differed significantly from that obtained in CD_3OD . This is suggested to be due to conformational changes taking place within the molecule. The most significant change was evident in Pro^2 C β and C γ , and the difference between these had decreased from 9.4 ppm in **1b** to 3.6 ppm in **1c** indicating a switch from the cis to the trans peptide bond geometry. These peptide bonds had changed from three cis prolines in CD_3OD (**1b**) to two cis and one trans in CDCl_3 (**1c**). An attempt to study the more polar conformer (**1a**) in CDCl_3 proved impossible due to its low solubility and complex spectra caused by multiple conformations.

TABLE 2. ^1H (δ /ppm, Proton Count, Multiplicity, J (Hz)), 400 MHz, ^{13}C (δ /ppm, Multiplicity), 100 MHz, and 2D NMR Data in CDCl_3 for Phakellistatin 2 Less Polar Conformer (**1c**)

no.	residue	atom	^{13}C	^1H	COSY $^1\text{H}-^1\text{H}$	HMBC C \rightarrow H
1	Phe	α	54.5 (d)	4.63(1H, m)	H1 β_A , H1 β_B , NH1	H1 β_A , H1 β_B
		β	37.3 (t)	A. 3.06 (1H, m) B. 2.72 (1H, m)	H1 α , H1 β_B H1 α , H1 β_A	H1 α , H1(2/6)
		1	135.6 (s)			H1(3/5), H1 β_A , H1 β_B
		2/6	130.4 (d)	7.12 (2H, d)	H1(3/5)	H1 β_A , H1 β_B
		3/5	130.0 (d)	7.24 (2H, d)	H1(2/6)	
		4	128.6 (d)	7.22 (1H, m)		H1(3/5)
		CO	172.4 (s)			H1 α
2	Pro	NH		8.46 (1H, d, 1.5)	H1 α	
		α	63.4 (d)	4.20 (1H, m)	H2 β_A , H2 β_B	
		β	30.4 (t)	A. 2.32 (1H, m) B. 1.88 (1H, m)	H2 α , H2 β_B H2 α , H2 β_A	H2 α
		γ	26.8 (t)	A. 2.11 (1H, m) B. 2.05 (1H, m)	H2 γ_B H2 γ_A	H2 α
		δ	48.0 (t)	A. 3.86 (1H, m) B. 3.81 (1H, m)	H2 δ_B H2 δ_A	H2 α
		CO	173.0 (s)			H2 α
		α	58.1 (d)	4.36 (1H, m)	H3 β , NH3	3 γCH_3
3	Ile	β	39.5 (d)	1.91 (1H, m)	H3 α	3 γCH_3
		γ	27.2 (t)	A. 1.60 (1H, m) B. 1.47 (1H, m)	H3 γ_B H3 γ_A	H3 α , 3 γCH_3
		γCH_3	14.9 (q)	0.91 (3H, m)	3 δCH_3	
		δCH_3	12.6 (q)	0.82 (3H, m)	3 γCH_3	
		CO	170.6 (s)			H3 α
		NH		6.65 (1H, d, 7.9)	H3 α	
		α	56.4 (d)	4.30 (1H, m)	H4 β , NH4	
4	Ile	β	40.8 (d)	1.67 (1H, m)	H4 α	H4 α , 4 γCH_3 , 4 δCH_3
		γ	23.0 (t)	A. 1.66 (1H, m) B. 1.52 (1H, m)	H4 γ_B H4 γ_A	H4 α , 4 γCH_3 , 4 δCH_3
		γCH_3	16.5 (q)	0.87 (3H, m)	4 δCH_3	
		δCH_3	13.2 (q)	0.96 (3H, m)	4 γCH_3	
		CO	172.1 (s)			H4 α
		NH		6.42 (1H, d, 9.3)	H4 α	
		α	62.4 (d)	4.49 (1H, d)	H5 β_A , H5 β_B	
5	Pro	β	32.8 (t)	A. 2.28 (1H, m) B. 2.07 (1H, m)	H5 α , H5 β_B H5 α , H5 β_A	H5 α H5 α
		γ	22.8 (t)	1.96 (1H, m) 1.86 (1H, m)	H5 γ_B H5 γ_A	H5 α
		δ	47.7 (t)	A. 3.54 (1H, m) B. 3.46 (1H, m)	H5 δ_B H5 δ_A	H5 α
		CO	170.2 (s)			H5 α
		α	55.6 (d)	4.37 (1H, m)	H6 β , NH6	
		β	39.1 (t)	2.95 (2H, m)	H6 α	H6 α , H6(3/5) H6(2/6)
		1	156.1 (s)			
6	Tyr	2/6	131.0 (d)	6.99 (2H, m)	H6(3/5)	
		3/5	116.2 (d)	6.64 (2H, m)	H6(2/6)	
		4	157.2 (s)			H6(2/5), H6(3/5)
		CO	170.6 (s)			H5 α
		NH		6.26 (1H, d, 4.8)	H6 α	
		α	61.4 (d)	3.11 (1H, m)	H7 β_A , H7 β_B	
		β	31.8	A. 1.85 (1H, m) B. 1.04 (1H, m)	H7 α , H7 β_B H7 α , H7 β_A	H7 α
7	Pro	γ	22.5 (t)	1.41 (1H, m) 0.83 (1H, m)	H7 γ_B H7 γ_B	H7 α
		δ	48.0 (t)	A. 3.46 (1H, m) B. 3.23 (1H, m)	H7 δ_B H7 δ_A	H7 α
		CO	172.1 (s)			H7 α

The initial isolation by Pettit of phakellistatin 2 showed an $\text{ED}_{50} = 0.34 \mu\text{g/mL}$ against P388 cells.¹¹ The activity was much reduced on subsequent screening, and this was attributed by others to a miss-assignment of structure, upon comparison to synthetic *cyclo*(Phe¹-Pro²-Ile³-Ile⁴-Pro⁵-Tyr⁶-Pro⁷).²³ It is obvious from the ^{13}C data for the Pro C β and C γ for this synthetic compound that this is in fact the trans/trans/cis Pro form and not the all-cis form originally found by Pettit. The C α shifts of this synthetic compound are also at variance with the originally isolated compound (Table 3). A re-synthesis by Pettit²⁴ obtained the all-cis Pro peptide bond geometry,

but the bioactivity was 2 orders of magnitude lower than the original isolation, P388 $\text{ED}_{50} = 24 \mu\text{g/mL}$, and this change was attributed to the fact that the initial isolate may have contained trace amounts of an additional, highly bioactive compound. A comparison of the C α shifts given in Table 3 indicates that the more polar conformer, **1a**, found during this study is in fact identical with that initially isolated and later re-synthesized by Pettit.¹¹ The less polar conformer, **1b**, in CD_3OD shows significant differences in several of the C α shifts, and this difference is accentuated when the compound is dissolved in CDCl_3 (**1c**). Given that the peptide sequences and absolute

TABLE 3. Comparison of the ^{13}C NMR Shifts of the C_α for All Residues in the Various Reported Phakellistatin Conformers

res	synthetic compd ²³	original isolate ¹¹	more polar conformer 1a (CD_3OD)	less polar conformer 1b (CD_3OD)	less polar conformer 1c (CDCl_3)
Pro ²	trans	cis	cis	cis	trans
Pro ⁵	trans	cis	cis	cis	cis
Pro ⁷	cis	cis	cis	cis	cis
1 Phe	56.5	55.6	55.3	53.0	54.5
2 Pro	61.6	62.3	62.0	62.2	63.4
3 Ile	59.7	59.9	59.5	59.6	58.1
4 Ile	56.4	55.8	55.4	58.3	56.4
5 Pro	60.4	63.3	62.9	62.5	62.4
6 Tyr	55.8	54.3	54.0	54.0	55.6
7 Pro	62.1	59.9	59.5	59.3	61.4

TABLE 4. Statistics for the Solution Structures Determined in This Study

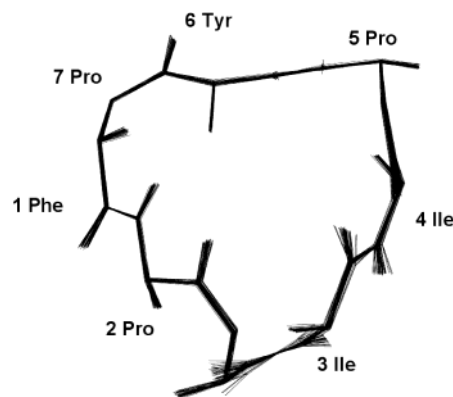
	more polar conformer 1a	less polar conformer 1b	less polar conformer 1c
solvent	CD_3OD	CD_3OD	CDCl_3
no. of NOE restraints	85	55	80
no. of structures refined (out of 100)	73	49	82
structures with the same BB (out of 100)	46	35	66
E_{tot} (kcal/mol)	10.6	14.2	13.7
BB RMSD (Å)	0.06 ± 0.02	0.06 ± 0.06	0.07 ± 0.04
heavy atom RMSD (Å)	0.38 ± 0.27	0.60 ± 0.25	0.80 ± 0.27

stereochemistry of the two phakellistatin 2 variants isolated in this study are found to be identical, the difference in their NMR spectra must be due to a difference in their solution conformations, and this was studied next.

Solution State Conformational Studies

Solution state conformations for both phakellistatin 2 conformers (**1a**, **1b**) were determined in CD_3OD and also for the less polar conformer in CDCl_3 (**1c**). ROE restraints were obtained from T-ROESY spectra ($T_{\text{mix}} = 300$ ms) and classified as weak (<5 Å), medium (<3.5 Å), or strong (<2.5 Å) (Tables S2, S6, and S10). Restrained molecular dynamics calculations were carried out using X-PLOR.²⁷ Statistics for the three structures are given in Table 4 and in the Supporting Information. All structures had low target energy functions and gave few restraint violations, and consensus structures (Figures 3, 5, and 7) had excellent backbone RMSD values. All ϕ and ψ angles were in the allowed regions of the Ramachandran diagram.²⁸

It can be seen that the major difference in conformations between the more polar conformer (**1a**, Figure 4) and the less polar conformer (**1b**, Figure 6) is the presence of the hydrogen bond between Phe¹-NH and Ile³-C=O in the latter (Figure 6). Several type IV β -turns can be found in the more polar conformer, between Phe¹-Ile⁴, Ile³-Tyr⁶, and Ile⁴-Pro⁷. The defining features for this type of 4-residue (i to $i + 3$) turn are that the distance from $\text{C}\alpha_i$ to $\text{C}\alpha_{i+3}$ is less than 7 Å and residues $i + 1$, $i + 2$ are nonhelical. The presence of an H-bond is not necessary for type IV β -turns.²⁹ The same four type IV β -turns can be identified in the less polar conformer **1b** (Figure 6),

**FIGURE 3.** Ensemble of 46 minimum energy structures of **1a** (more polar conformer) in CD_3OD (backbone only shown).

and in addition an H-bond is also present between Phe¹-NH and Ile³-C=O, although this does not follow the usual β -turn hydrogen bonding pattern of $\text{C}=\text{O}_i$ to NH_{i+3} . The dissolution of the less polar conformer of **1b** in CDCl_3 brings about a drastic change in conformation, with the most obvious change being *cis*-Pro² to *trans*-Pro² (**1c**, Figure 8). Again, three type IV β -turns can be identified, this time Phe¹-Ile⁴, Pro²-Pro⁵, and Ile⁴-Pro⁷. A hydrogen bond now from Phe¹-C=O to Ile³-NH defines an inverse γ -turn with ϕ_{i+1} and ψ_{i+1} angles of -91.5° and 58.4° , respectively, compared to the ideal values of -79° and 69° .²⁹

The independent stability of the two conformers of **1** in CD_3OD may be attributed to a relatively large barrier to their interconversion. A calculation of their accessible surface areas gives a value of 983 Å^2 for the more polar conformer (**1a**) and 944 Å^2 for the less polar conformer

(27) Brunger, A. T. *X-PLOR a system for X-ray crystallography and NMR 3.851*; Yale University: New Haven, CT, 1993.

(28) Laskowski, R. A.; MacArthur, M. W.; Moss, D. S.; Thornton, J. M. *J. Appl. Crystallogr.* **1993**, *26*, 283–291.

(29) Hutchinson, E. G.; Thornton, J. M. *Protein Sci.* **1996**, *5*, 212–220.

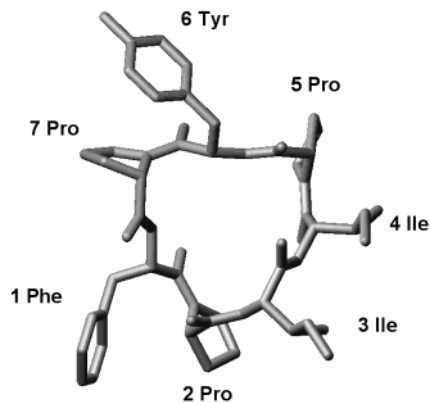


FIGURE 4. Representative minimum energy structure of **1a** (more polar conformer) in CD_3OD (heavy atoms only shown).

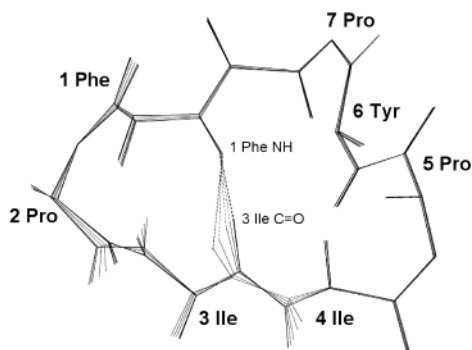


FIGURE 5. Ensemble of 35 minimum energy structures of **1b** (less polar conformer) in CD_3OD (backbone only shown) showing the hydrogen bond.

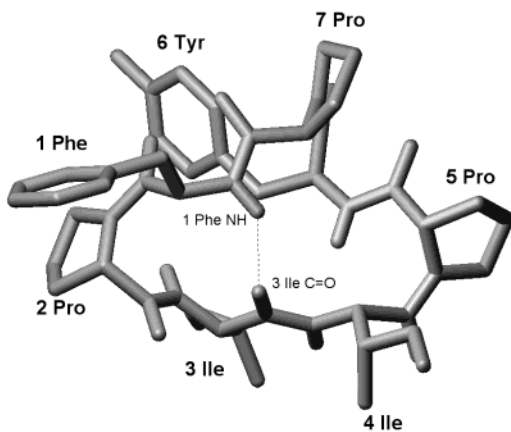


FIGURE 6. Representative minimum energy structure of **1b** (less polar conformer) in CD_3OD (heavy atoms only shown) showing the hydrogen bond.

(**1b**).³⁰ This difference of 39 \AA^2 of buried surface area will give an additional 4.1 kJ mol^{-1} stabilization for the less polar conformer (**1b**), in addition to which it receives an additional $3\text{--}5 \text{ kJ mol}^{-1}$ stabilization due to the presence of an H-bond.³¹ The total stabilization of the less polar conformer (**1b**) relative to the more polar **1a** is therefore in the order of $7\text{--}9 \text{ kJ mol}^{-1}$, which is enough to allow

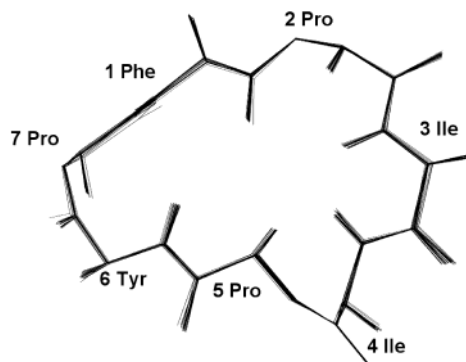


FIGURE 7. Ensemble of 35 minimum energy structures of **1c** (less polar conformer) in CDCl_3 (backbone only shown).

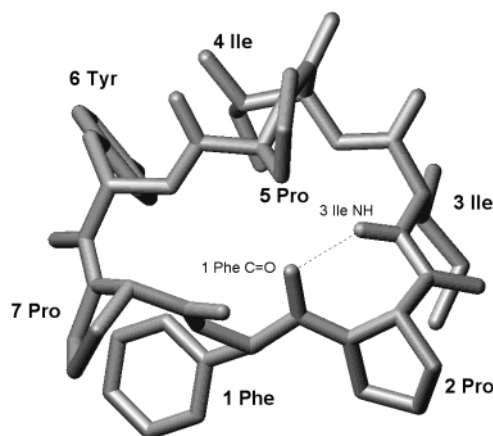


FIGURE 8. Representative minimum energy structure of **1c** (less polar conformer) in CDCl_3 (heavy atoms only shown) showing the hydrogen bond.

TABLE 5. IC_{50} Values in $\mu\text{g/mL}$ against K562 Leukaemia Cells and A2780 Ovarian Tumor Cells for the Two Phakellistatin Conformers Isolated during This Work

	more polar conformer 1a		less polar conformer 1b	
solvent	DMSO	MeOH	DMSO	MeOH
K562	33.02		> 50.0	
A2780	28.27	2.72	> 50.0	1.12
K562 ^a		> 50.0		> 50.0
A2780 ^a		34.81		45.39

^a Assay conducted 8 weeks later.

both conformations to exist independently at room temperature.

Conclusions

It can be seen that a change in solvent polarity from CD_3OD (dielectric 32.7) to CDCl_3 (dielectric 4.8) causes a large change in conformation (Figures 6 and 8). However, the difference in conformations observed in CD_3OD (Figures 4 and 6) is similarly large and is due mainly to the disruption of one hydrogen bond between $\text{Phe}^1 \text{NH}$ and $\text{Ile}^3 \text{C=O}$, and is consistent with the observed change in retention time in HPLC.

The two conformers of the phakellistatins isolated during this work were tested against K562 leukaemia cells and A2780 ovarian tumor cells (Table 5). As can be seen, the activity is highly dependent on the solvent and

(30) Koradi, R. M. B.; Wuthrich, K. *J. Mol. Graph.* **1994**, *14*, 51–59.

(31) Chotia, C. *Annu. Rev. Biochem.* **1984**, *53*, 537–572.

the time the sample is left in the solvent before the assay is conducted. The most common MTT cytotoxicity assay solvent is the polar aprotic solvent DMSO (dielectric constant = 46.9). The assay was also conducted in the polar protic solvent MeOH (dielectric = 32.7). The greatest activity was observed in MeOH, comparable to that obtained during the initial isolation by Pettit.¹¹

The suggestion is that the less polar conformer, **1b**, is the one originally isolated with high cytotoxicity. The stability of the less polar conformer, **1b**, is due to a combination of factors as described above. In addition, the disruption of the Phe¹ NH–Ile³ C=O H-bond present in the less polar conformer in CD₃OD, with concomitant loss of bioactivity, is slow due to the very effective hydrophobic shielding from the solvent of the two groups involved in the H-bond. The amino acid residues in phakellistatin 2 are all moderately (Pro, Tyr) to strongly (Phe, Ile) hydrophobic and would provide a very effective shield from the solvent.

Experimental Section

General. HPLC was performed using an ODS 10 μ m spherical particle/100 Å pore size column and UV detection at 254 nm. All NMR spectra were recorded with a 400 MHz instrument at 26 °C in CDCl₃ using residual CHCl₃ as an internal reference at 7.27 ppm. All mass spectrometry was carried out at the Department of Biomolecular Mass Spectrometry, Universiteit Utrecht, Utrecht, The Netherlands. HRMS were obtained on a quadrupole-time-of-flight instrument with electrospray ionization. In addition ESI-MS was used to observe fragmentations followed by MSⁿ work using an ion trap mass spectrometer in electrospray ionization mode. All samples were dissolved in HPLC grade methanol.

Collection. The sample of *Stylotella aurantium* (collection number 9712SD140) was collected in December 1997 at a depth of about 5 m by snorkelling from *Cakaulevu* reef, in the district of *Wainunu*, in the island of *Vanua Levu*, Fiji Islands (17° 2.609'; 178° 54.694' E). The sample was identified by John Hooper of the Queensland Centre for Biodiversity and voucher specimens are held at the South Pacific Herbarium, University of the South Pacific, Fiji, and at the Marine Natural Products Laboratory, University of Aberdeen, Scotland, UK.

Extraction and Isolation. All sponges were extracted and partitioned by standard procedures as previously described.³² The dichloromethane fraction was subjected to Sephadex size exclusion chromatography (LH-20) with a mixture of methanol and dichloromethane (50/50) as eluent. Similar fractions were pooled on the basis of TLC analysis. Analysis by ¹H and ¹³C NMR indicated that one pooled fraction contained small peptides. This fraction was given priority for isolation work. Purification was achieved by reversed-phase C18 HPLC with a mixture of acetonitrile, water, and trifluoroacetic acid (50/50/0.1) as eluent to give axinellin C, pseudoaxinellin (9.2 mg), phakellistatin 2 (**1a**, 6.6 mg), its less polar conformer (**1b**, 9.5 mg), and wainunuamide (11.2 mg).

Phakellistatin 2 More Polar Conformer (1a). Colorless oil, 6.6 mg (0.00040%) yield; [α]_D²⁵ –74.1° (c 0.001 MeOH); UV (100% MeOH) λ_{\max} 280 (log ϵ 3.50); IR (cm^{–1}) LR ESI-MS *m/z* 828.4 [M + H]⁺, 850.4 [M + Na]⁺ and HR ESI-MS 850.4421 [M + Na]⁺ Δ 0.0 mmu from that calculated for C₄₂H₆₂O₈N₇; NMR data in Table S1.

Phakellistatin 2 Less Polar Conformer (1b). Colorless oil, 9.5 mg (0.00060%) yield; [α]_D²⁵ –53.1° (c 0.001 MeOH); UV (100% MeOH) λ_{\max} 280 (log ϵ 3.53); IR (cm^{–1}) 1687, 1651, 1517, 1448, 1346, 1261, 1187, 1044; LRESIMS *m/z* 828.4 [M + H]⁺, 850.4 [M + Na]⁺ and HREIMS 828.4594 [M + H]⁺ Δ

0.7 mmu, 850.4410 [M + Na]⁺ Δ 1.1 mmu from that calculated for C₄₂H₆₂O₈N₇; NMR data in Table 1 (CD₃OD) and Table 2 (CDCl₃).

Absolute Stereochemistry. (a) Acid Hydrolysis. Each cyclic peptide and the relevant amino acid standards were hydrolyzed with 3–4 mL of 6 M HCl at constant boiling at 110 °C for 18 h and then dried on a rotary evaporator. The hydrolysate was reconstituted in 2.0 mL of 0.1 M HCl and 20 μ L was pipetted and dried under vacuum. To this was added 10 μ L of redrying solution consisting of a mixture of ethanol, water, and triethylamine (2.0/2.0/1.0) and then the mixture was redried as before.

(b) Chiral TLC. The amino acids were analyzed by chiral TLC using reverse-phase chiral plates (ODS impregnated with a proline derivative and Cu²⁺) with a mixture of methanol, water, and acetonitrile (1:1:4) as the solvent system and detected by ninhydrin spray reagent.³³ The stereochemistry of each of the amino acid residue was found to be L.

Structure Calculation. Restraints were derived from the T-ROESY spectrum (*T*_{mix} = 300 ms) and classified as weak, medium, or strong by contour counting (Tables S2, S6, and S10). In all cases the lengths of restraints for methyl residues were extended by 0.5 Å to allow for the differential relaxation of methyls. Restrained molecular dynamics calculations were carried out with XPLOR 3.851²⁷ using a force field with repulsive nonbonded terms. Ab initio simulated annealing calculations (YASAP 3.0: 120 ps total time simulated annealing from 2000 to 100 K, 200 steps of minimization) were used to calculate structures from 100 starting conformations with randomized ϕ and ψ angles. From this ensemble structures were refined using a simulated annealing with slow cooling protocol (600 ps, cooling from 1500 to 100 K, 4000 steps of minimization). The lowest energy structures from the ensemble were selected to represent the final structure. The overlay and display of structures was achieved with Molmol.³⁰

Cell Cytotoxicity Testing. To determine the effect of **1a** and **1b** on cell lines, a semiautomated cytotoxicity assay was employed. The assay is a quantitative colorimetric one using a tetrazolium salt, originally described by Mossmann,³⁴ and has the advantage of being rapid, precise, and semiautomatic. The assay measures the ability of viable cells to reduce MTT (3-(4,5-dimethylthiazol-2-yl)-2,5-diphenyl tetrazolium bromide), a yellow tetrazolium salt, to a purple formazan precipitate. This process known as metabolic reduction requires active mitochondrial function to reduce the salt. Viable cells take up the tetrazolium salt and metabolize it to insoluble formazan crystals which are localized within the cells and can be visualized under light microscopy. The medium and non-reduced MTT is aspirated from the cells and the formazan solubilized in DMSO, and the resulting solution is read using a spectrophotometer. Using a 96 well plate format absorbance was found to be directly proportional to the number of cells in each well, and the linearity extended over almost the entire range tested, i.e. from 200 to 50 000 cells/well.

(a) 96 Well Assay. The standard assay for cytotoxicity employed a 96 well format, using between 400 and 1000 cells per well in 100 μ L. Each drug dose was represented by three wells. A 100- μ L sample of media containing doubling dilutions of 2 \times drug was added to triplicate sets. Control wells received 100 μ L of medium alone. The plates were then incubated in a humidified atmosphere for 5 days at 37 °C, with 5% CO₂. After incubation 50 μ L of MTT solution (3 mg/mL) was added to each well and the plate returned to the incubator for 3 h. After incubation the medium and excess MTT was aspirated from each well and the formazan crystals solubilized in 200 μ L of DMSO. The plate was then read using a multiscan microplate reader (Titertech) at 540 nm with subtraction at 620 nm to

(32) Morris, L. A.; Kettenes-van den Bosch, J. J.; Versluis, K.; Thompson, G. S.; Jaspars, M. *Tetrahedron* **2000**, *56*, 8345–8353.

(33) Gunther, K.; Martens, J.; Schickedanz, M. *Angew. Chem., Int. Ed. Engl.* **1984**, *23*, 506.

(34) Mossmann, T. *J. Immunol. Methods* **1983**, *63*, 55–66.

allow for turbidity. The resultant output was processed using an excel spreadsheet. The percentage growth inhibition ((mean absorbance of drug treated wells/mean absorbance of control well) \times 100) and IC_{50} (concentration of compound required to inhibit 50% growth) were calculated.

Acknowledgment. J.N.T. would like to thank Ratu Isoa Bulikiobo for permission to collect samples and Usaia Tabudravu and Inosa Qatavi for sample collections. J.N.T. wishes to thank the University of the South Pacific, the Government of Fiji, and the ORSAS (UK)

for financial support. L.A.M. was a PDF supported by BBSRC grant no. 1/E12737. Kees Versluis is thanked for accurate mass measurements.

Supporting Information Available: NMR data for **1a**, tables of restraints, restraint violations, energies, and structure ensemble statistics for **1a**, **1b**, and **1c**, and details of the structure calculation protocol. This material is available free of charge via the Internet at <http://pubs.acs.org>.

JO020482S